J Mater Sci (2010) 45:1588–1594
DOI 10.1007/s10853-009-4129-9

Size-controlled recrystallization of fullerene by gas–antisolvent process

**Shunsuke Mochizuki · Akira Teramoto ·
Fuyuko Yamashita · Yasuhiko Kasama ·
Yoshiyuki Sato · Hiroshi Inomata**

Received: 26 July 2009 / Accepted: 13 December 2009 / Published online: 29 December 2009

Abstract Gas–antisolvent (GAS) process using CO_2 successfully prepared crystals of fullerene (C_{60}) from a toluene solution through a precipitation. Particle sizes of precipitated C_{60} could be easily controlled by changing the initial pressurization rate of CO_2, the temperature at the initial pressurization, and the quantity of C_{60}. Fullerene particles obtained by GAS method had regular octahedral shapes, whereas the particles obtained by adding liquid ethanol as an antisolvent to C_{60} solution did not have such shape. Particle sizes could be changed in a range of 1.0–8.5 μm by GAS method; they were wider than the range of particles obtained by ethanol addition (0.7–1.8 μm).

Introduction

Fullerene is an attractive material known as a new stable form of carbon with unique physical and chemical properties. Since Krätschmer et al. [1] discovered the electric arc method for the synthesis of fullerene in large amounts, many studies have suggested useful applications of fullerenes for superconductivity, optical and electronics materials, catalysts, and pharmaceutical industry [2–5]. In these applications, fullerene derivatives suitable for the respective use are necessary; however, the preparation of derivatives often faced difficulty because of the low solubilities of fullerenes in various organic solvents [6, 7]. Although aromatic solvents such as toluene can dissolve fullerene, they are toxic to biological systems. Recently, methods for producing fine suspensions of fullerene have been attractive for the synthesis of fullerene derivatives [8–13]. These methods are based on the control of the dissolving power of fullerene solution by adding an antisolvent. Masuhara et al. [14] reported the preparation of fullerene fine crystals from a fullerene solution by using some combinations of a solvent and an antisolvent. They revealed the important factors that control the size of fullerene crystals such as the concentration of the fullerene in solution, the aging temperature after precipitation; various combinations of organic solvents and antisolvents gave significant effects on the size and shape of fullerene crystals. This process had a success in controlling the morphology of fullerene particles by using organic solvents. On the contrary, by using the solvent and antisolvent, their separation at the end of the process requires the use of energy. Moreover, organic solvents usually cause problems to both the environment and health.

Here, we would like to focus on the utilization of the supercritical fluid to prepare fullerene crystals. Recrystallization methods using supercritical CO_2 ($scCO_2$) have been studied to be an alternative technique to the conventional process using organic solvents. CO_2 is inert and nontoxic; thus, waste problems of solvent can be excluded. The following methods employ a supercritical fluid: rapid expansion of supercritical solutions (RESS) [14], aerosol solvent extraction system (ASES) [15, 16], and gas–antisolvent (GAS) process [17, 18]. In RESS method, the supercritical solution containing a target compound is rapidly expanded into a low pressure environment, and this leads to a large supersaturation and precipitation to produce particles of the compound. When a target compound has

S. Mochizuki · A. Teramoto · Y. Sato · H. Inomata (✉)
Graduate School of Engineering, Research Center
of Supercritical Fluid Technology, Tohoku University, Aramaki
Aza Aoba 6-6-11-403, Aoba-ku, Sendai 980-8579, Japan
e-mail: inomata@scf.che.tohoku.ac.jp

F. Yamashita · Y. Kasama
Ideal Star Inc., ICR Bldg 6-6-3, Minamiyoshinari, Aoba-ku,
Sendai 989-3204, Japan

very low solubility in a supercritical fluid, the ASES and GAS methods are used; the supercritical fluid acts as an antisolvent. In ASES method, a liquid solution containing a target compound is sprayed into a supercritical phase. The droplets of the solution expand rapidly, and the particles are precipitated from the liquid solution. In the GAS method, a dense gas is dissolved to a liquid solution containing a compound. The liquid phase is expanded by increasing the gas density, and the dissolving power of the solution decreases. This leads to precipitate particles of the compound. The solvent can be easily removed within the flow of supercritical fluid.

Among supercritical fluid processes, the RESS method is not suitable for the recrystallization of fullerene because the solubility of fullerene in $scCO_2$ is negligibly small [19, 20]. In contrast with the RESS method, ASES and GAS methods can be applied. To date, using supercritical fluid to recrystallize fullerene particles has been reported with $scCO_2$ or other materials [21, 22]. Although preparations of fullerene particles were successful with supercritical fluid, the systematic study concerning the factor deciding the size of particles is insufficient. In this article, we report a preparation of the fullerene crystal by GAS method with $scCO_2$, and the factors controlling the size of particles are described in detail. The GAS method showed a characteristic advantage to control the contact rate of the antisolvent CO_2 compared with the conventional method using liquid antisolvent.

Experimental

Materials

Fullerene (C_{60} (99.5%)) was obtained from Aldrich and used without further purification. Toluene and ethanol were reagent grade of Wako Pure Chemical Industries, Ltd. The fullerene solution was prepared by dissolving fullerene particles into toluene with ultrasonic treatment for 30 min. Concentrations of fullerene in toluene solutions were 0.5 or 1 g/L. Prepared sample solutions were stored in a dark place.

Recrystallization of fullerene by GAS method

Experimental studies were carried out by a conventional supercritical fluid extraction system [23]. A 1–15 mL of fullerene solution dissolved in toluene was loaded into an extraction cell (volume: 34 mL). The cell was immersed in an oven (Shimadzu GC-8A, 40–60 °C) and kept at the target temperature for 1 h. The initial pressurization rate up to the saturated vapor pressure of CO_2 was adjusted at the range of 0.05–0.6 MPa/s by manually handling a valve. Then the cell was pressurized with CO_2 (99.9%) to 15 MPa with a flow rate of 4 mL/min at an HPLC pump (JASCO 880-PU, head temperature was 2 °C). Toluene and CO_2 were completely mixed at this condition [24]. The CO_2 was flowed into the cell at 2 mL/min of a flow rate for 1 h (at 2 °C on the pump and system pressure) and/by allowing the back pressure regulator (JASCO 880-81) to control the system pressure. The solvent toluene was separated from the outlet CO_2 stream by depressurization and collected in a separation vial. After flowing for 1 h, the cell was finally depressurized, and then residual powders in the cell were collected.

Characterization

The shape of fullerene crystals obtained was analyzed by scanning electron microscopy (SEM, JEOL JSM-6390) without any coating treatment. Particle sizes and size distributions were calculated by ImageJ [25] from obtained SEM images. IR spectra of fullerene were obtained on a JASCO FT-IR-230. Powder X-ray diffraction patterns of fullerene particles were analyzed on a Rigaku MiniFlex (CuK_α radiation, $\lambda = 1.5405$ Å).

Results and discussion

Morphology and properties of C_{60} crystals obtained by GAS method

The raw C_{60} before dissolution in toluene appears as aggregates of various sizes and shapes (Fig. 1a). These C_{60} particles generate a purple solution in toluene. A simple drying of this purple solution by air blow gave a powder of C_{60}, where aggregates of particles of various sizes were also present (Fig. 1b). In comparison with those particles, C_{60} particles obtained by GAS method had an octahedral shape with regular size (Fig. 1c). These results show that a simple drying process of the liquid C_{60} solution can easily cause the cohesion of C_{60} particles due to the surface tension of the solvent, whereas GAS method with $scCO_2$ can eliminate the influence because the liquid solvent is removed without generating its surface by dissolving into $scCO_2$ phase. The characteristic octahedral shape of C_{60} crystals obtained by the GAS method may be concerned with the coexisting solvents, toluene, and CO_2. It is known that crystals of C_{60} generated from solutions form solid solvates [26]; C_{60} recrystallized from toluene solution includes one or two toluene molecules in the unit cell of the corresponding crystals [27]. In a recrystallization experiment of C_{60} from a toluene solution by adding 2-propanol as an antisolvent, a unique star-like shape was also reported [14]. In addition, C_{60} has been reported to form gas

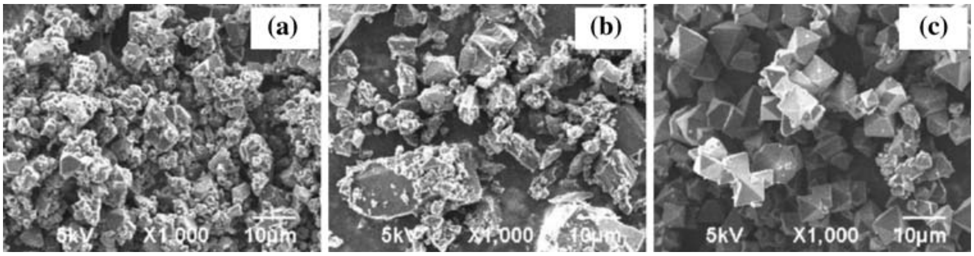

Fig. 1 SEM images of C_{60}. **a** Raw material of C_{60} before GAS treatment, **b** solid obtained from a toluene solution of C_{60} by drying with air blow, **c** C_{60} crystals obtained by GAS method (40 °C, 15 MPa, sample: 0.5 g/L, 14 mL)

inclusion crystals as $C_{60}(CO_2)_x$ in a recrystallization with $scCO_2$ as the antisolvent [21]. Although the coexisting solvent seems to have a significant effect on deciding the shape of C_{60} crystals, the relationship between the octahedral shape and solvents used in this study is as yet unclear. On the contrary, the presence of CO_2 in the obtained crystals was confirmed by FT-IR measurement. Figure 2 shows FT-IR spectra of raw C_{60} and C_{60} crystals obtained by GAS method. In comparison with the spectrum of raw C_{60} (Fig. 2a), a strong band at 2372 cm^{-1} (pointed by an arrow) appears in the crystals obtained by the GAS method (Fig. 2b). This band was assigned to the antisymmetric stretching mode of CO_2 and indicated the existence of CO_2 molecules in the crystals. In order to get other qualitative information on C_{60} crystals prepared by the GAS method, we performed powder XRD measurements. Figure 3 shows powder X-ray diffraction patterns for raw C_{60} and C_{60} particles obtained by GAS (2θ values for raw C_{60} (Fig. 3a: 10.6, 17.4, 20.5, 21.5, 27.2, 27.9, 30.7, 32.6); for C_{60} by GAS (Fig. 3b): 10.5, 17.4, 20.5, 21.4, 22.3, 27.2, 27.9, 30.6, 32.5). Differences in 2θ values of predominant peaks between raw C_{60} and C_{60} crystals by GAS were very small. An obvious difference was found at the peak (2θ value = 22.3) for C_{60} by GAS as shown in Fig. 3b. Previous reports describing the formation of $C_{60}(CO_2)_x$ with XRD measurement did not show such peak [21]. The origin of that peak in this study may be related to toluene; however, it remains an unclear phenomenon. Although crystal structures for raw C_{60} and C_{60} by GAS seemed to be similar, further investigation will be necessary to reveal the shape and structure of the crystals.

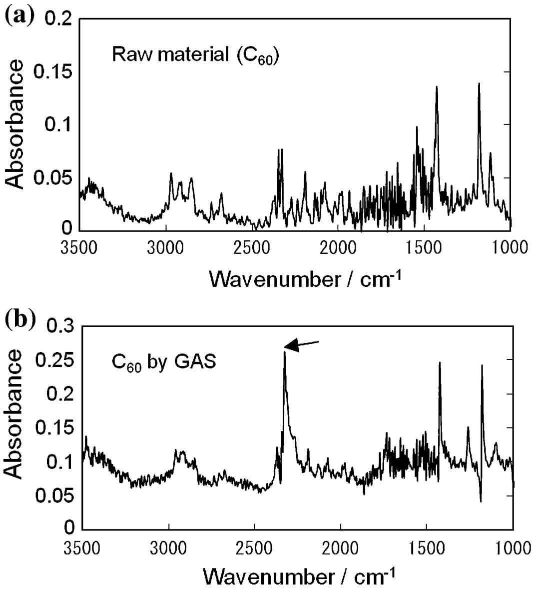

Fig. 2 FT-IR spectra of C_{60}. **a** Raw C_{60}, **b** C_{60} by GAS method. The sample **b** was the same material shown in Fig. 1c. The *arrow* indicates the peak assigned to the antisymmetric stretching mode of CO_2

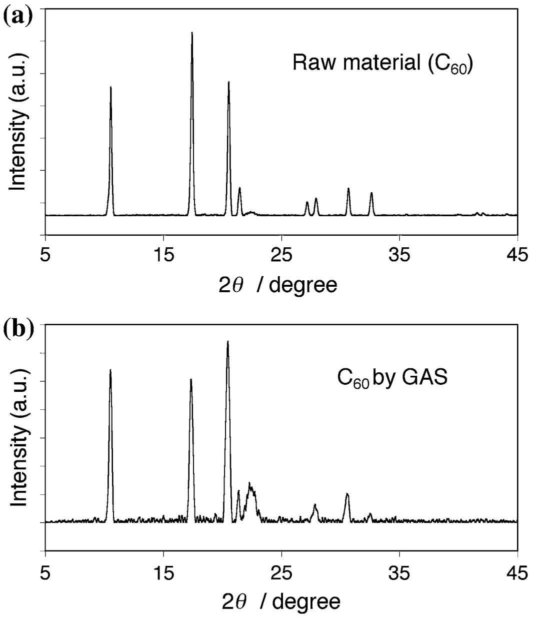

Fig. 3 Powder X-ray diffraction patterns for C_{60}. **a** Raw C_{60}, **b** C_{60} by the GAS method. The sample **b** was the same material shown in Fig. 1c

Size-controlled recrystallization of C_{60} particles

In the conventional method using a solvent and an antisolvent to recrystallize C_{60}, the place where the antisolvent contacts with the solvent is important in the generation and growth of crystals. A rapid mixing of the antisolvent will cause a rapid supersaturated state to produce small crystals of C_{60}. For the same reason, a rapid pressurization of CO_2 as the antisolvent into C_{60} toluene solution will generate small crystals. This was confirmed by changing the initial pressurization rate in GAS method. Figure 4 shows the effect of that rate on the size of generated particles. Relatively low pressurization rate (0.1 MPa/s, Fig. 4a) gave larger crystals (average particle size: 4.9 µm), while the faster pressurization rates (0.4 and 0.6 MPa/s for Fig. 4b, c, respectively) gave smaller crystals (average particle size: 3.0 and 1.7 µm for Fig. 4b, c, respectively).

It was found that the temperature at the initial pressurization of the GAS treatment cell had a strong effect on determining the size of C_{60} particles under a constant pressurization rate (0.1 MPa/s). Figure 5 shows the effect of those temperatures on the size of C_{60} particles. In these experiments, temperatures at the GAS treatments were not the same; 40 °C for Fig. 5a, c, and 60 °C for Fig. 5b. The procedure to obtain the result of Fig. 5c was as follows: the cell was initially cooled by ice, and then pressurized to the pressure of CO_2 cylinder (ca. 5.6 MPa). Next, the temperature of the cell was elevated to 40 °C for the GAS treatment and the cell was pressurized to 15 MPa. A comparison between Fig. 5a (40 °C) and b (60 °C) indicates that lower temperatures favored the formation of small particles. The particle size was obviously decreased by decreasing the temperature at the initial pressurization; the smallest particles were obtained at the lowest temperature (Fig. 5c, average particle size: 1.0 µm).

Both the effect of the pressurization rate and the temperature at initial pressurization can be related with the dissolving behavior of CO_2 into C_{60} toluene solution. The slower pressurization allows crystal growth by the slow reducing of the dissolving power of the C_{60} toluene solution. The faster pressurization would bring about a rapid precipitation before crystal growth through a rapid reduction of the dissolving power of toluene, and it leads to generation of smaller particles. On the effect of the temperature at the initial pressurization, the solubility of CO_2 into toluene is promoted at the lower temperature [28]. This would cause the same effect on the crystal growth as indicated in the effect of pressurization rate. Although the solubility of C_{60} in toluene increases by decreasing the temperature [29, 30], the effect seems to be smaller than the effect of high solubility of CO_2 in toluene at a low temperature.

Another factor that determines the size of C_{60} crystals by the GAS method was found to be the quantity of C_{60}. Figure 6 shows the effect of the volume of the sample solution on the size of particles. The concentration of C_{60} in solutions was constant (1 g/L). The particle sizes of C_{60} increased by increasing the volume of sample solution

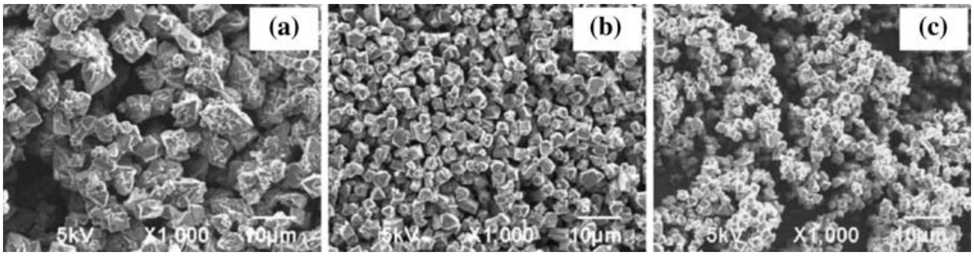

Fig. 4 SEM images of C_{60} crystals obtained by GAS method (sample: 1 g/L, 3 mL, GAS treatment: 40 °C, 15 MPa) with various initial pressurization rates. Pressurization rates were **a** 0.1 MPa/s, **b** 0.4 MPa/s, and **c** 0.6 MPa/s, respectively. Average particle sizes were **a** 4.9 µm, **b** 3.0 µm, and **c** 1.7 µm, respectively

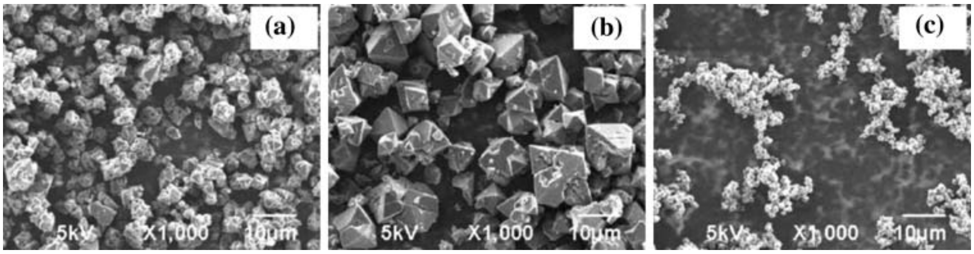

Fig. 5 SEM images of C_{60} crystals obtained by GAS method (sample: 1 g/L, 1 mL, initial pressurization rate: 0.1 MPa/s, GAS treatment: pressure was 15 MPa, temperature was 40 °C for **a** and **c**, 60 °C for **b**, respectively) with various temperatures at initial CO_2 introducing. Temperatures were **a** 40 °C, **b** 60 °C, and **c** iced, respectively. Average particle sizes were **a** 3.3 µm, **b** 8.1 µm, and **c** 1.0 µm, respectively

from 1 mL (Fig. 6a) to 15 mL (Fig. 6c). Figure 7 shows the effect of the concentration of C_{60} in the solution on the size of particles. The volume of the sample solution was 1 mL; concentrations of C_{60} were 1 g/L (Fig. 7a) and 0.5 g/L (Fig. 7b). It was indicated that the particle size was obviously increased by increasing the concentration of C_{60} in the solution (Fig. 7b). Both these results shown in Figs. 6 and 7 can be related to the amount of C_{60} in the recrystallization process. Namely, the increase of the absolute quantity of C_{60} would enhance the crystal growth.

On the contrary, the particle size was not sensitive to the pressure at the GAS treatment. Figure 8 shows the effect of the pressure on the size of particles. The average particle size ranged only from 3.0 to 3.9 μm at various pressures. In contrast to the effect of initial pressurization rate (Fig. 4) or the temperature at initial pressurization (Fig. 5), the influence of the pressure at the GAS treatment was small on changing the size of particles. This suggests that the particle generation occurred rapidly at the initial CO_2 introduction and the particle size was determined at this state. For example, the C_{60} particles were already observed at the bottom in the cell when the C_{60} solution was pressurized to 2–3 MPa and rapidly depressurized without GAS treatment. This shows that the generation of C_{60} particles rapidly occurred upon introduction of CO_2.

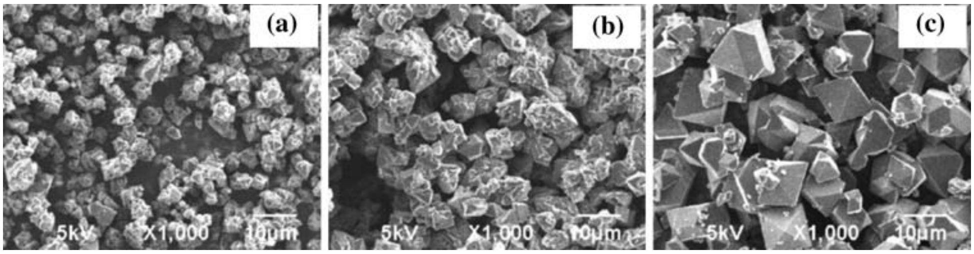

Fig. 6 SEM images of C_{60} crystals obtained by GAS method (sample: 1 g/L, initial pressurizing rate: 0.1 MPa/s, GAS treatment: 40 °C, 15 MPa) with various volume of sample solution. Volumes were **a** 1 mL, **b** 3 mL, and **c** 15 mL, respectively. Average particle sizes were **a** 3.3 μm, **b** 4.9 μm, and **c** 8.5 μm, respectively

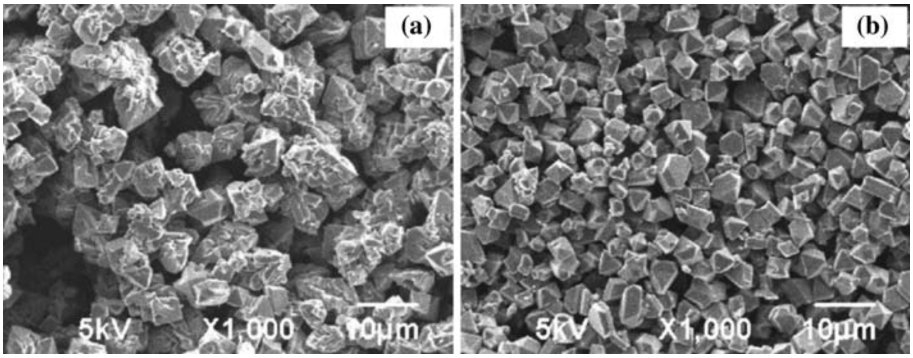

Fig. 7 SEM images of C_{60} crystals obtained by GAS method (initial pressurizing rate: 0.1 MPa/s, GAS treatment: 40 °C, 15 MPa, sample: 1 mL) with various concentration of C_{60}. Concentrations were **a** 1 g/L, **b** 0.5 g/L. Average particle sizes were **a** 4.9 μm, **b** 3.6 μm, respectively

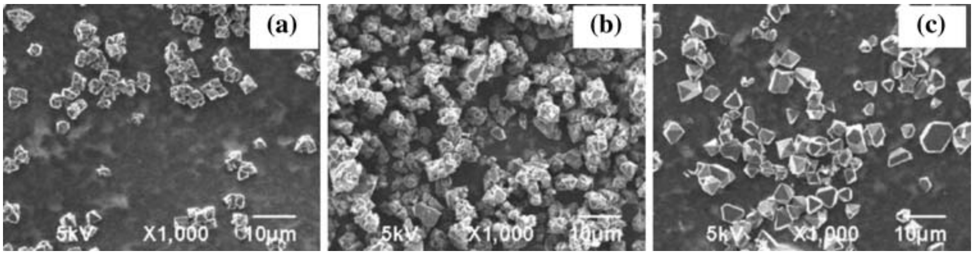

Fig. 8 SEM images of C_{60} crystals obtained by GAS method (sample: 1 g/L, 1 mL, initial pressurizing rate: 0.1 MPa/s, GAS treatment: 40 °C, 15 MPa) with various pressure at the GAS treatment. Pressures were **a** 10 MPa, **b** 15 MPa, and **c** 20 MPa, respectively. Average particle sizes were **a** 3.0 μm, **b** 3.3 μm, and **c** 3.9 μm, respectively

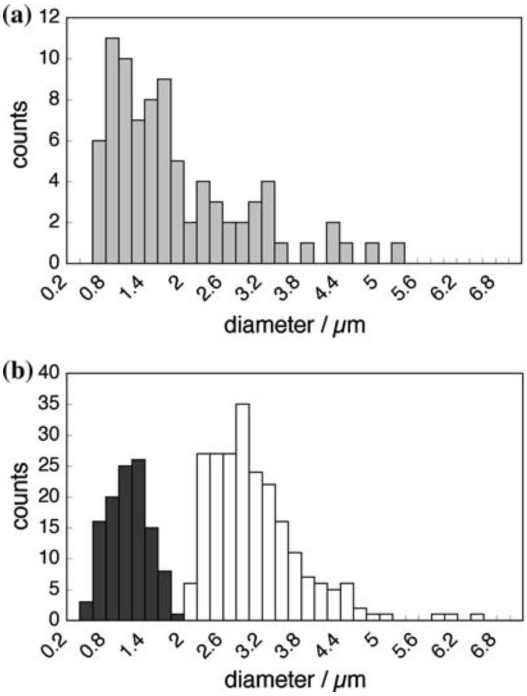

Fig. 9 Size distributions of particles for C_{60}. **a** Raw material of C_{60} before GAS treatment, **b** C_{60} crystals obtained by GAS method. Black bars: data of Fig. 3c, white bars: data of Fig. 3a

Figure 9 shows the comparison in the distribution of the particle size between raw C_{60} and particles obtained by GAS method. The data of GAS method were two results shown in Figs. 3a, c. It is clearly shown that narrow distributions of C_{60} particles were obtained by GAS method.

Comparison with recrystallization using organic solvent

A recrystallization using organic solvents was compared to the GAS method. Here, ethanol was selected as the antisolvent. In this section, two types of experimental conditions were examined: a rapid mixing of C_{60} toluene solution into ethanol (method A), and slow titration (1 droplet/3–5 s) of ethanol into C_{60} toluene solution (method B). These two processes were regarded to correspond to the effect of initial pressurization rate in the GAS method (results shown in Fig. 4).

Figure 10 shows C_{60} particles generated from the mixing of ethanol and C_{60} toluene solution. In contrast to the results by GAS method, the shape of particles obtained was not octahedral. The average particle size by method A (rapid mixing) was 0.7 μm; it was smaller than that by GAS method (1.0 μm was the smallest in GAS method). Method B (slow titration) also gave small particles having the average particle size 1.8 μm. The obvious differences in the particle size as shown in Fig. 10 indicated that the mixing rate of solvent and antisolvent certainly controlled the particle size, as shown in Fig. 4.

In our experiments, the smallest particle was obtained not by the GAS method but with ethanol; however, the particle sizes could be widely controlled by the GAS method (1.0–8.5 μm) than with ethanol (0.7–1.8 μm).

Conclusions

Particles of C_{60} were successfully prepared by the GAS method with CO_2. Factors controlling the size of particles were determined through changing the initial pressurization rate, the temperature at initial pressurization, and the quantity of C_{60}. The effective dissolution of CO_2 into C_{60} solution gave smaller particles, and the increase in concentration of C_{60} promoted crystal growth. Size distributions of the obtained particles were narrow compared with that of raw C_{60}.

The method using organic solvent gained superiority to GAS method on producing smaller particles; however, the reuse of the solvent is not easy because the complete separation of the solvent and antisolvent is necessary. The GAS method provides the ease of reuse of the solvent by simple depressurization of supercritical CO_2. The GAS method may contribute to prepare fullerene particles for various applications.

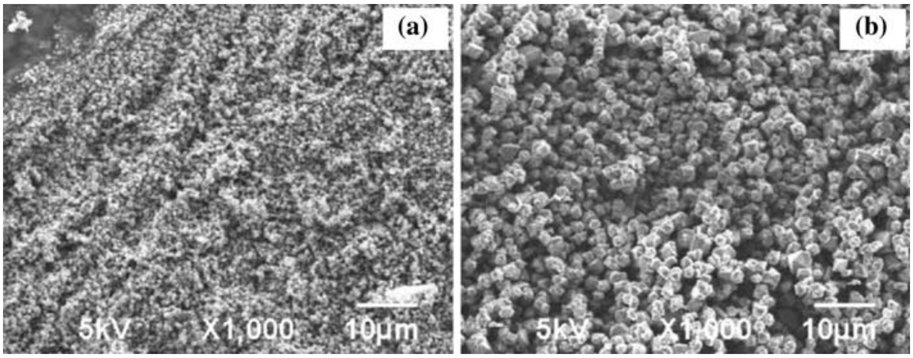

Fig. 10 SEM images of C_{60} crystals obtained by adding ethanol as the antisolvent (sample: 1 g/L, 0.5 mL, ethanol: 1 mL). **a** Method A (rapid mixing), **b** Method B (slow titration). Average particle sizes were **a** 0.7 μm, **b** 1.8 μm

References

1. Krätschmer W, Lamb LD, Fostiropoulos K, Huffman DR (1990) Nature 347:354
2. Yildirim T, Barbedette L, Kniaz K, Fischer JE, Lin CL, Bykovetz N, Stephens PW, Sulewski PE, Erwing SC (1995) Mater Res Symp Proc 359:273
3. Wang Y (1992) Nature 356:585
4. Joutsensaari J, Ahonen P, Tapper U, Kauppinen EI, Laurila J, Kuokkala VT (1996) Synth Met 77:85
5. Wei Z, Jinke T, Puri A, Seany RL, Yuxin L, Liquan C (1996) J Mater Res 11:2749
6. Marcus Y (1997) J Phys Chem B 101:8617
7. Abraham MH, Green CE, Acree EA Jr (2000) J Chem Soc Perkin Trans 2:281
8. Dhawan A, Taurozzi JS, Pandey AK, Shan W, Miller SM, Hashsham SA, Tarabara VV (2006) Environ Sci Technol 40:7394
9. Khokhryakov AA, Kyzyma OA, Bulavin LA, Len A, Avdeev MV, Aksenov VL (2007) Crystallogr Rep 52:487
10. Deguchi S, Yamazaki T, Mukai S, Usami R, Horikoshi K (2007) Chem Res Toxicol 20:854
11. Deguchi S, Mukai S (2006) Chem Lett 35:396
12. Alargova RG, Deguchi S, Tsuji K (2001) J Am Chem Soc 123:10460
13. Tan Z, Masuhara A, Kasai H, Nakanishi H, Oikawa H (2008) Jpn J Appl Phys 47:1426
14. Masuhara A, Tan Z, Kasai H, Nakanishi H, Oikawa H (2009) Jpn J Appl Phys 48:050206
15. Charoenchaitrakool M, Dehghani F, Foster NR, Chan HK (2000) Ind Eng Chem Res 39:4794
16. Bustami RT, Chan HK, Dehghani F, Foster NR (2000) Pharm Res 17(11):1360
17. Bleich J, Müller BW, Waßmus W (1993) Int J Pharm 97:111
18. Warwick B, Dehghani F, Foster NR, Biffin JR, Regtop HL (2000) Ind Eng Chem Res 39:4571
19. Dehghani F, Foster NR (2003) Curr Opin Solid State Mater Sci 7:363
20. Saim S, Kuo KC, Stalling DL (1993) Sep Sci Technol 28:1509
21. Field CN, Hamley PA, Webster JM, Gregory DH, Titman JJ, Poliakoff M (2000) J Am Chem Soc 122:2480
22. O'Neil A, Wilson C, Webster JM, Allison FJ, Howard JAK, Poliakoff M (2002) Angew Chem Int Ed 41:3796
23. Mochizuki S, Wada N, Smith RL Jr, Inomata H (1999) Analyst 124:1507
24. Ng HJ, Robinson DB (1978) J Chem Eng Data 23:325
25. Abramoff MD, Magelhaes PJ, Ram SJ (2004) Biophotonics Int 11:36
26. Keita B, Nadjo L, Céolin R, Agafonov V, André D, Szwarc H (1994) Chem Phys 179:595
27. Korobov MV, Stukalin EB, Mirakyan AL, Neretin IS, Slovokhotov YL, Dzyabchenko AV, Ancharov AI, Tolochko BP (2003) Carbon 41:2743
28. Lay EN, Taghikhani V, Ghotbi C (2006) J Chem Eng Data 51:2197
29. Ruoff RS, Malhotra R, Huestis DL, Tse DS, Lorents DC (1993) Nature 362:140
30. Sawamura S, Fujita N (2007) Carbon 45:965